microbial biotechnology

Open Access

Glycine significantly enhances bacterial membrane vesicle production: a powerful approach for isolation of LPS-reduced membrane vesicles of probiotic *Escherichia coli*

Satoru Hirayama[1,2] and Ryoma Nakao[1]*

[1]*Department of Bacteriology I, National Institute of Infectious Diseases, 1-23-1 Toyama, Shinjuku, Tokyo, 162-8640, Japan.*

[2]*Japan Agency for Medical Research and Development, 20F Yomiuri Shimbun Bldg. 1-7-1 Otemachi, Chiyoda, Tokyo, 100-0004, Japan.*

Summary

Bacterial membrane vesicles (MVs) have attracted strong interest in recent years as novel nanoparticle delivery platforms. Glycine is known to induce morphological changes in the outer layer of bacteria. We report here that glycine dramatically facilitates MV production in a flagella-deficient mutant of the non-pathogenic probiotic *Escherichia coli* strain Nissle 1917. Supplementation of culture medium with 1.0% glycine induced cell deformation at the early exponential phase, eventually followed by quasi-lysis during the late exponential to stationary phase. Glycine supplementation also significantly increased the number of MVs with enlarged particle size and altered the protein profile with an increase in the inner membrane and cytoplasmic protein contents as compared to non-induced MVs. Of note, the endotoxin activity of glycine-induced MVs was approximately eightfold or sixfold lower than that of non-induced MVs when compared at equal protein or lipid concentrations respectively. Nevertheless, glycine-induced MVs efficiently induced both immune responses in a mouse macrophage-like cell line and adjuvanticity in an intranasal vaccine mouse model, comparable to those of non-induced MVs. We propose that the present method of inducing MV production with glycine can be used for emerging biotechnological applications of MVs that have immunomodulatory activities, while dramatically reducing the presence of endotoxins.

Received 25 December, 2019; revised 21 March, 2020; accepted 22 March, 2020.
*For correspondence. E-mail ryoma73@nih.go.jp; Tel. (+81) 3 5285 1111; Fax (+81) 3 5285 1150.
Microbial Biotechnology (2020) **13**(4), 1162–1178
doi:10.1111/1751-7915.13572
Funding information
This study was supported by a grant from the Japan Agency for Medical Research and Development (AMED, no. JP18fk0108124) and JSPS KAKENHI (JP16K11537, JP18K15160, JP19H02920 and JP19K22644).

Introduction

During various phases of growth, bacteria produce membrane vesicles (MVs) that contain much of the biological content derived from their parent bacterial cells, such as phospholipids, lipopolysaccharides (LPS), proteins, enzymes, toxins, DNA and RNA (Kaparakis-Liaskos and Ferrero, 2015). MVs are anticipated to have a wide range of applications in medical and healthcare settings (Toyofuku *et al*., 2015; Wang *et al*., 2015). In particular, MVs are now attractive as a potential proteoliposomal carrier of vaccines (van der Pol *et al*., 2015), thanks to the advantages of nano-sized admixtures, their immunological properties and their structural stability. On the other hand, the benefit of their potent immunogenicity and adjuvanticity must be weighted against their safety and reactogenicity (often related to LPS in MVs) in the context of risk/benefit in vaccine design (Boutriau *et al*., 2007; van der Ley and van den Dobbelsteen, 2011). Therefore, the development of a novel MV vaccine platform that can achieve protective immunity without side-effects is highly desirable.

Escherichia coli Nissle 1917 (EcN) is the most commonly used Gram-negative probiotic strain and is marketed in several countries as the drug product Mutaflor (Ardeypharm, Herdecke, Germany) (Behnsen *et al*., 2013), where it is widely used to treat enteric diseases, including infectious diarrhoea and inflammatory bowel disease in humans (Rembacken *et al*., 1999; Kruis *et al*., 2004). EcN cells compete with enteric pathogens in the murine gut via microcin secretion (Sassone-Corsi *et al*., 2016). In addition, EcN cells and their MVs enhance the host cell-mediated immune response, and modulate the balance between pro- and anti-inflammatory cytokines (Behnsen *et al*., 2013; Fabrega *et al*., 2016). EcN MVs have also been shown to induce self-adjuvanted protective humoral immune responses in a mouse model

(Rosenthal *et al*., 2014); thus, they have also drawn attention for their potential utility as antigen carriers in humans.

Glycine is frequently used as a food additive in many countries, because of its sweetness, low cost, high solubility in water and safety in humans (Shibasaki, 1982; European Commission, 2014; U.S. Food and Drug Administration, 2018). Glycine also has an antibacterial effect via inhibiting peptidoglycan (PG) synthesis by substitution of glycine for DL-alanine of PG during bacterial growth (Hammes *et al*., 1973; de Jonge *et al*., 1996). By using this PG-weakening effect, glycine has also been utilized for genetic transformation (Beringer, 1974; Holo and Nes, 1989; Thompson and Collins, 1996; Ito and Nagane, 2001; Larsen *et al*., 2007) and spheroplast formation (Chatterjee and Williams, 1963; John and Russell, 1963; Sato *et al*., 1966).

MV productivity differs among bacterial species and strains, and that variability of productivity is an important consideration to be addressed for practical applications of MVs. Although the mechanism of MV formation has not been fully elucidated, several models have been presented. For example, MVs might be induced by PG endopeptidase activity and/or accumulation of substances such as PG fragments in the periplasm (Schwechheimer and Kuehn, 2015). In addition, McBroom *et al*. demonstrated that disruption of some genes related to PG synthesis enhanced MV production in *E. coli* (McBroom *et al*., 2006). Recently, a novel mechanism of MV formation by 'explosive' cell lysis was proposed, which is initiated by the action of a phage-derived peptidoglycan-degrading enzyme, endolysin (Turnbull *et al*., 2016; Toyofuku, 2019). From these findings, we hypothesized that glycine, which has a PG-weakening effect, can facilitate bacterial MV production. In the present study, we report that glycine can be utilized to easily and efficiently enhance production of flagella-free MVs from the culture supernatant of an EcN derivative. Moreover, glycine-induced and non-induced MVs have been morphologically and immunologically characterized in both in vitro and in vivo assays. Notably, glycine-induced MVs could elicit strong immune responses at levels comparable to those of non-induced MVs, despite dramatically reduced endotoxin activity. Here, we discuss the broad applicability of glycine-induced MVs as a novel drug delivery platform in medical and healthcare settings.

Results

Construction of flagella-deficient EcN mutant and isolation of flagella-free MVs

In the present study, we chose the probiotic strain EcN as an MV producer for prospective MV application because of its established safety in humans (Rembacken *et al*., 1999; Kruis *et al*., 2004). MV fractions prepared from EcN wild-type strain were heavily contaminated with flagella, which also strongly adhered to the MVs (Fig. 1A). In order to isolate flagella-free MVs from EcN, the MV preparation was first subjected to density gradient centrifugation. However, this purification method was not suitable for EcN MVs, as the separation method not only failed to completely remove flagella from the MV preparations, but also dramatically decreased the MV yield (data not shown), which was in agreement with a published report (Chutkan *et al*., 2013). To completely exclude flagella from the MV preparation without any sample loss, we constructed a non-polar *flhD* deletion mutant (EcNΔ*flhD*) that lacks the flagellar transcriptional activator FlhD. Whole cells of EcNΔ*flhD* did not express any flagellin FliC (Fig. S1), and thus, flagella-free pure MVs were successfully isolated using a simple, one-step approach by ultracentrifugation of the culture supernatant (Fig. 1A and B). We did not observe significant differences regarding MV morphology between the EcN and isogenic EcNΔ*flhD* strains (Fig. 1A). Furthermore, SDS-PAGE analysis results revealed no obvious difference in the protein profile of the MVs between these strains, except for the absence of a sharp band corresponding to FliC in the MV preparations of the EcNΔ*flhD*, as anticipated (Fig. 1B).

On the other hand, we unexpectedly observed some differences in the whole-cell protein profiles ranging from 15 to 20 kDa (Fig. S1), though the reason for those remains unclear. Nevertheless, given that the synthesis and operation of flagella require significant energy (Soutourina and Bertin, 2003), it is not surprising that minor changes in the protein profile occur as a result of *flhD* mutation. We have also found some filamentous structures thinner than the flagella in the MV preparations from both the EcN and EcNΔ*flhD* strains (Fig. 1A, white arrowheads), which is in good agreement with a previous proteomic study of MV preparations from EcN strain, in which some fimbrial proteins were detected (Aguilera *et al*., 2014).

Glycine induced quasi-lysis during stationary phase

A growth assay was performed to evaluate the effect of glycine on cell growth of the EcNΔ*flhD* strain. The EcNΔ*flhD* was aerobically cultured in Luria–Bertani (LB) broth supplemented with or without glycine at different concentrations (Fig. 2A). Exponential-phase growth was inhibited in a dose-dependent manner by glycine supplemented at final concentrations of 1.2%, 1.5% and 2.0%, but not by lower glycine concentrations of 0.5% and 1.0% (Fig. 2A). However, the OD values significantly dropped at the stationary phase over time, when 1.0% glycine was used (Fig. 2A). Morphologically, all

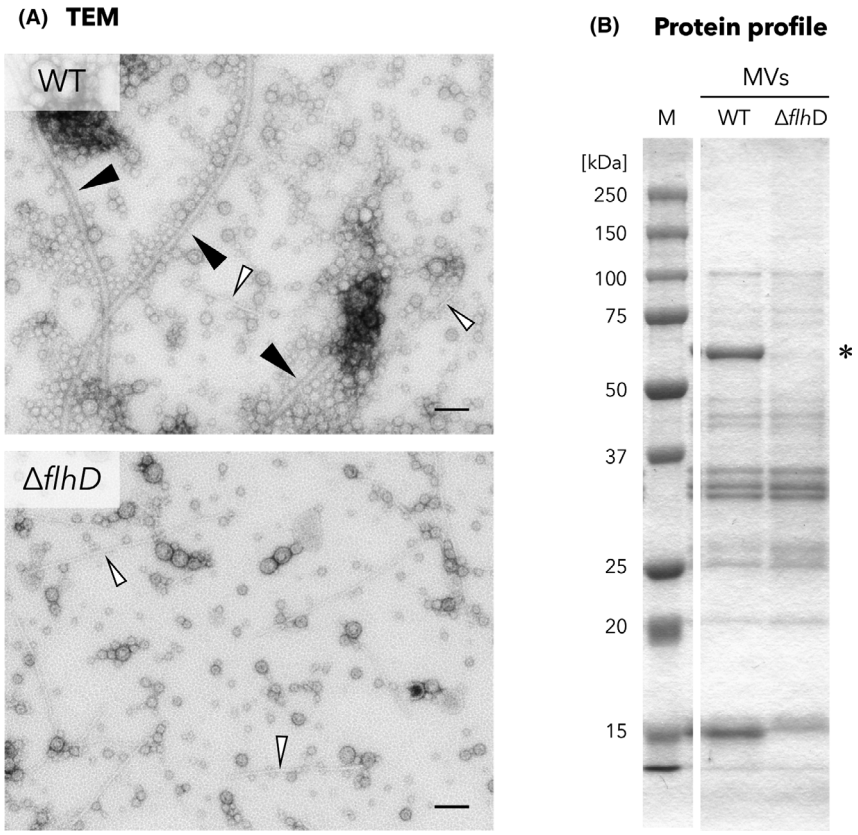

Fig. 1. Characterization of EcNΔ*flhD* mutant.
A. TEM images of MV fractions of EcN wild type (WT) and the Δ*flhD* mutant (Δ*flhD*). The samples were diluted to a protein concentration of 150 and 60 ng μl^{-1}, respectively, for observation. Black arrowheads and white arrowheads denote flagella and fimbriae respectively. Scale bars represent 100 nm.
B. Protein profiles of MV preparations from WT and Δ*flhD*. MV samples were analysed by SDS-PAGE using 12.5% polyacrylamide gels and stained with CBB. The same MV protein amounts were loaded into each lane. 'M' represents the marker (precision plus protein all blue standards, Bio-Rad, Hercules, CA). Asterisk denotes FliC.

EcNΔ*flhD* cells were deformed when cultured in the presence of 1.0% glycine for at least 3 h (Fig. 2B). The whole cells of EcNΔ*flhD* cultured in 1.0% glycine-supplemented LB broth appeared as spindle-like, distorted rods at 3 h (Fig. 2B). The morphological abnormality caused by 1.0% glycine further progressed with the longer incubation (6 h) (Fig. 2B). Some cells were finally broken at 16 h (Fig. 2B), whereas no broken or deformed cells were found under non-induced conditions at the same time points (Fig. 2B). These data clearly indicated that supplementation with 1.0% glycine deformed the cell structure despite a normal exponential growth curve, which was followed by quasi-lysis during the stationary growth phase.

Glycine significantly enhanced MV production

SEM data also showed emergence of large membrane blebs on the cell surface, as well as large MVs released from the cells when cultured for 6 and 16 h in 1.0% glycine-supplemented LB broth (red arrowheads, Fig. 2B and C). In addition, more small MVs were produced under glycine-induced conditions, and the number of small MVs increased especially at 16 h (yellow arrowheads, 'Gly', Fig. 2C), while fewer small MVs were produced under non-induced conditions (yellow arrowheads, 'N', Fig. 2C). The dramatic increase in MV production was confirmed by the pellet formation following ultracentrifugation of culture supernatants of EcNΔ*flhD* (EcNΔ*flhD*; Fig S2). We obtained similar results in the case of another *E. coli* laboratory strain (BW25113 Δ*flhD*; Fig S2). Some MVs were shown to be with filamentous structures (white arrowheads, Fig. 2C), as also seen in TEM analysis (Fig 1A).

We then employed different qualitative approaches for MVs, which revealed that protein or lipid amounts increased 69- or 51-fold, respectively, by supplementation with 1.0% glycine (Table 1). Normalized by corresponding OD_{600} value, both of protein and lipid amounts increased in a dose-dependent manner due to addition

Table 1. Comparison the amounts of MVs between non-induced and glycine-induced conditions by different qualitative approaches

	Non-induced conditions (N)	Glycine-induced conditions (Gly)	Fold change (Gly/N)
Protein amount [mg]	0.028 ± 0.0042	1.9 ± 0.22	69
Lipid amount [mg]	0.17 ± 0.040	8.5 ± 0.99	51
LPS amount [EU]	$(0.87 \pm 0.26) \times 10^6$	$(7.0 \pm 0.63) \times 10^6$	8.1

Shown are the data of non-induced (N) and glycine-induced MVs (Gly) with fold change (Gly/N) of the values of the respective parameters. The values of protein, lipid, and endotoxin are indicated as the amount in MVs collected from a 70 ml culture. Each value represents mean ± standard error of three independent experiments.

of glycine (0–1.5%) (Fig. S3). A glycine concentration of 2.0% was considered to be a critical level to severely inhibit growth (Fig. 2A), resulting in low yield of MVs (Fig. S3). The particle size of glycine-induced MVs distributed wider than that of non-induced MVs, and the mean diameter of glycine-induced MVs (mean ± SD: 36.3 ± 15.0 nm) was significantly greater than that of non-induced MVs (28.2 ± 9.54 nm) (Fig. 3A–C). Of note, regardless of the quasi-lysis that occurred in the glycine-supplemented conditions (Fig. 2B), the percentage of MV with abnormal morphology, which was defined as irregular, shrunken and/or flattened membranous structures instead of rounded structures, was only 1.36% (Fig. 3D). There was no significant difference in the ratio of abnormal MVs to total MVs between non-induced and glycine-induced conditions (Fig. 3D).

Compositional changes in MVs due to glycine supplementation

Next, non-induced and glycine-induced MVs standardized by protein concentration were subjected to SDS-PAGE to compare their protein profiles. The overall protein profile of glycine-induced MVs was similar to that of non-induced MVs (Fig. 4A). However, a few bands showed obvious differences in their densities. For example, the density of the protein band found at 15 kDa was significantly higher in non-induced MVs as compared to glycine-induced MVs (denoted as #1, Fig. 4A). Two different fimbrial proteins, FimA and FocG, were identified as the two most abundant proteins of the #1 band (Table 2).

On the contrary, the protein band found at 100 kDa was significantly higher in glycine-induced MVs as compared to non-induced MVs (denoted as #2 in Fig 4A). Acetaldehyde dehydrogenase, AdhE, was identified as the most abundant protein in the #2 band. Although *E. coli* AdhE is known to be involved in anaerobic metabolism (Clark and Cronan, 1980) and gene regulation (Beckham *et al*., 2014), the physiological role of extracellularly released AdhE remains unknown. The PSORTb program predicted the protein to be localized in cytosol (Table 2).

Western blotting using antisera against subcellular marker proteins indicated that the expression level of the outer membrane protein OmpC in non-induced MVs was equivalent to that in glycine-induced MVs (Fig. 4B). In contrast, the expression levels of the inner membrane protein RodZ and the cytosolic protein Crp were markedly increased in glycine-induced MVs (Fig. 4B), which is in good agreement with the finding of enhanced expression of AdhE, another cytosolic protein (Fig. 4A and Table 2). All three subcellular marker proteins in whole-cell lysates collected from the respective culture conditions were detected at similar levels, ruling out the possibility that expression of RodZ and Crp increased at the cellular level (Fig. 4B).

Regarding LPS amounts in MVs, we compared the total endotoxin activities between non-induced and glycine-induced MVs, which are collected from the same volume of the culture supernatant. Surprisingly, the total LPS amounts in glycine-induced MVs to non-induced MVs were only 8.1-fold (Table 1), which stands in

Fig. 2. Growth and morphology of whole cells and MVs of EcNΔ*flhD* strain in the absence or presence of glycine.
A. Growth curves of the EcNΔ*flhD* in the absence or presence of glycine at different concentrations. Error bars represent standard error of the mean of three independent experiments. The growth curves were generated by sequential measurement of OD at 660 nm. The cells tended to aggregate when LB broth was supplemented with 1.5% glycine, which is denoted by an asterisk (*).
B. Whole cells of EcNΔ*flhD* cultured in the absence or presence of glycine. The EcNΔ*flhD* was cultured with shaking for 3, 6 and 16 h in LB without [non-induced conditions (N), top panels] or with 1.0% glycine [glycine-induced conditions (Gly), bottom panels]. Shown are four representative SEM images of cell appearance at each time point. Red arrowheads show the emergence of large membrane blebs on the bacteria. Scale bars represent 1 μm.
C. MVs of EcNΔ*flhD* cultured in the absence or presence of glycine. SEM images of MVs of the EcNΔ*flhD* cultured for 3, 6 and 16 h in LB without (N) or with 1.0% glycine (Gly). Red, yellow and white arrowheads denote large MVs, small MVs and fimbriae respectively. Scale bars represent 50 nm.

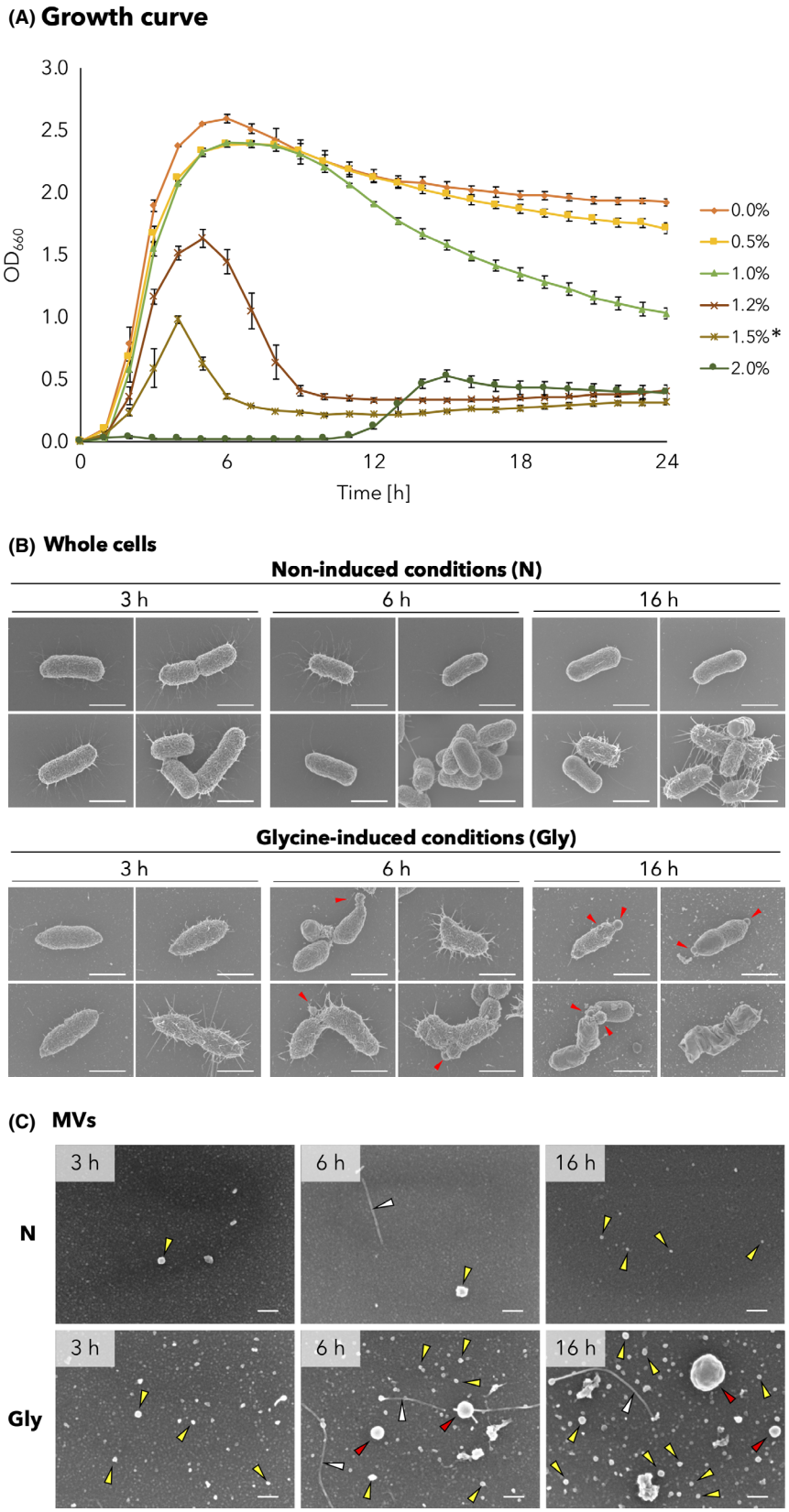

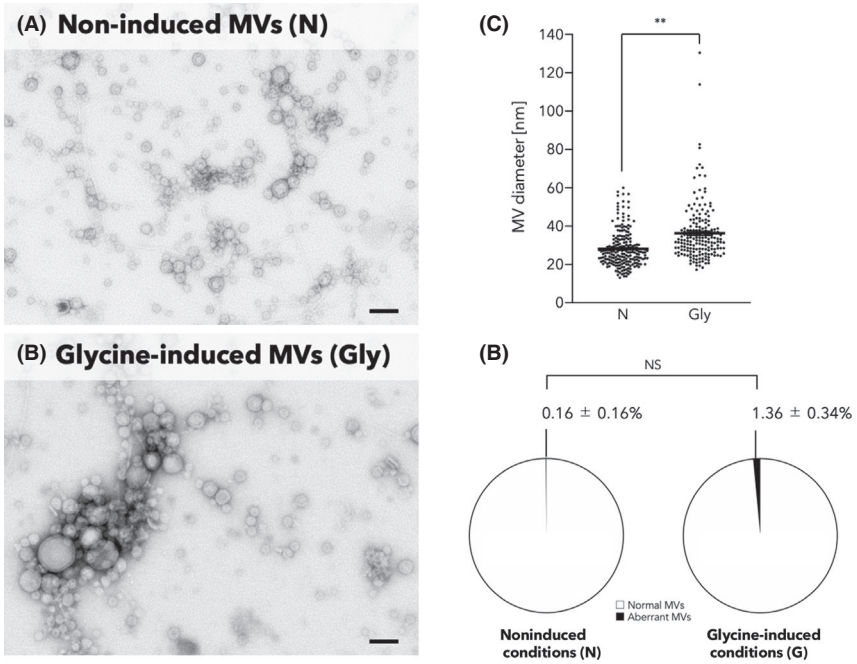

Fig. 3. Difference in morphology between non-induced MVs and glycine-induced MVs.
A and B. TEM images of MV fractions of the EcNΔ*flhD* cultured in LB media without (A) and with 1.0% glycine (B). The samples standardized at a protein concentration of 60 ng μl^{-1} were analysed by TEM. Scale bars represent 100 nm.C. Distribution of the size of MVs. Horizontal bars represent mean values. Statistical analysis was performed using a Mann–Whitney's *U*-test (*N*, $n = 213$; Gly, $n = 181$; $^{**}P < 0.01$).D. Percentage of aberrant MV numbers to total MV numbers. The number of MVs with aberrant morphology was calculated by counting the number of MVs with aberrant morphology in three randomly extracted 1.1×1.4 μm^2 TEM images. MV with aberrant morphology was defined as irregular, shrunken and/or flattened membranous structures instead of rounded structures. The mean percentages with standard errors of aberrant MVs to total MVs are indicated on the pie charts. Statistical analysis was performed using unpaired *t*-test with Welch's correction (triplicate experiments, NS: not significant).

marked contrast to the higher-fold changes in protein (69-fold) or lipid amounts (51-fold) (Table 1). As a result, the amount of LPS in glycine-induced MVs was approximately eightfold or sixfold lower than that in non-induced MVs, following standardization based on the amount of total protein (Fig. 4C) or total lipid (data not shown) respectively. This dramatic reduction in LPS amounts in glycine-induced MVs was also confirmed by SDS-PAGE, following application of silver staining and Western blotting using anti-*E. coli* LPS O6 antiserum (Fig. 4C). In the silver stain findings, two different types of LPS species were detected, semi-rough and rough, which were

Table 2. Identification of two representative bands of MV proteins

Rank[a]	Name	Locus Tag[b]	MASCOT score[a]	Theoretical pI/MW[c]	Subcellular localization[d]	Lipoprotein signal peptide[e]	Signal peptide [f]
Band ID #1 at 15 kDa							
1	Type-1 fimbrial protein subunit A, FimA	ECOLIN_05555	480	5.12/ 15873.56	Extracellular	No	Yes/24
2	Type-1 fimbrial protein protein G precursor, FocG	ECOLIN_05580	244	8.66/ 15187.76	Non-cytoplasm	No	Yes/22
3	Outer membrane lipoprotein, SlyB	ECOLIN_08845	202	8.93/ 15627.66	Outer membrane	Yes/17	No
Band ID #2 at 100 kDa							
1	Acetaldehyde dehydrogenase	ECOLIN_07285	1134	6.32/ 96058.13	Cytoplasm	No	No

a. The list of proteins is ranked by MASCOT score. All candidates with MASCOT score greater than 200 and more than two peptide hits.
b. Locus tags in the whole genome database of *Escherichia coli* Nissle 1917 (NCBI DB Accession: CP007799.1).
c. Theoretical pI/molecular weight predicted by ExPaSy.
d. Cellular localization predicted by PSORTb 3.02 program.
e. Presence/length of lipoprotein signal peptides predicted by LipoP 1.0 program.
f. Presence/length of signal peptides predicted by SignalP 4.1 program. Total peptide numbers are also shown in parentheses.

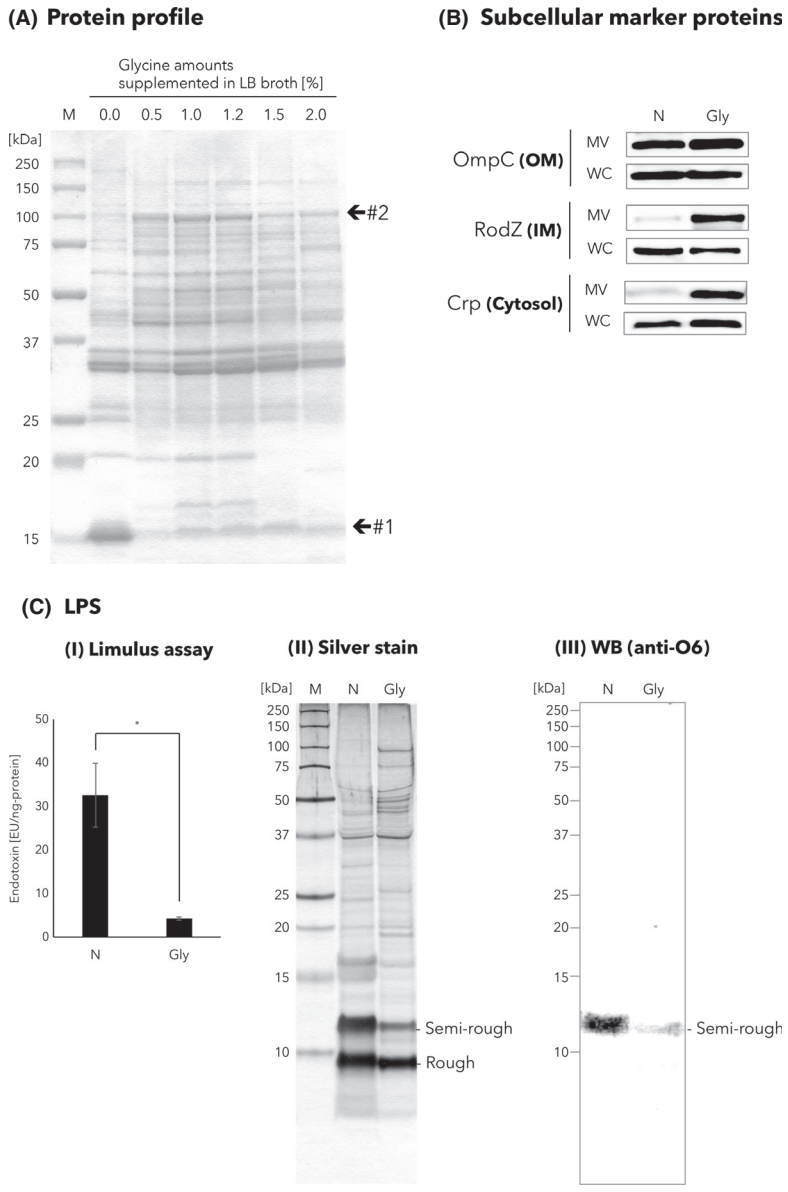

Fig. 4. Analysis of the amounts of subcellular marker proteins and LPS.
A. Protein profiles of MVs isolated in different culture conditions, in which the LB broth contained different amounts of glycine (0–2.0%). The same amount of protein (1.7 μg) was loaded into each lane of the SDS-PAGE. Locations of bands #1 and #2 in the CBB-stained SDS-PAGE gel are indicated. See also Table 2, in which the results of protein identification of these bands are shown. 'M' represents marker.
B. Analysis of subcellular marker proteins. Western blotting analyses of OmpC, RodZ and Crp proteins in MV and whole-cell (WC) samples prepared from LB media supplemented without (N) or 1.0% glycine (Gly). The same amount of protein was loaded into each lane.
C. LPS analyses of MVs. (I) Limulus assay. The amount of LPS in glycine-induced and non-induced MVs. Shown are the mean values with standard errors of the endotoxin unit (EU) following standardization with the protein amounts (ng). Statistical analysis was performed using unpaired *t*-test with Welch's correction ($n = 3$, $^*P < 0.05$). (II) Silver stain. Protein profiles of non-induced and glycine-induced MVs of EcNΔ*flhD* were assessed by silver staining. The same amount of protein was loaded into each lane. MV samples were separated by Tris-Tricine SDS-PAGE using 16.5% polyacrylamide gels and stained with silver nitrate. (III) WB [anti-O6]. The same amount of protein was loaded into each lane. MV samples were separated by Tris-Tricine SDS-PAGE using 16.5% polyacrylamide gels. LPS O6 antigen in the MV samples was probed with *E. coli* O6 antiserum. A single nucleotide mutation is located in the *wzy* gene (encodes O-antigen polymerase) of the O6 antigen synthesis gene cluster in the chromosome of the EcN strain (Grozdanov *et al*., 2002). Due to the single nucleotide exchange in the *wzy* gene, EcN LPS lacks long O-antigen. Shown are two different LPS species, a semi-rough-type (Semi-rough) and rough-type (Rough), composed of lipid A-core oligosaccharide with and without a single O-antigen repeating unit respectively (Grozdanov *et al*., 2002). Hence, only semi-rough species that contain one unit of O6 oligosaccharide are detectable with anti-O6 antiserum.

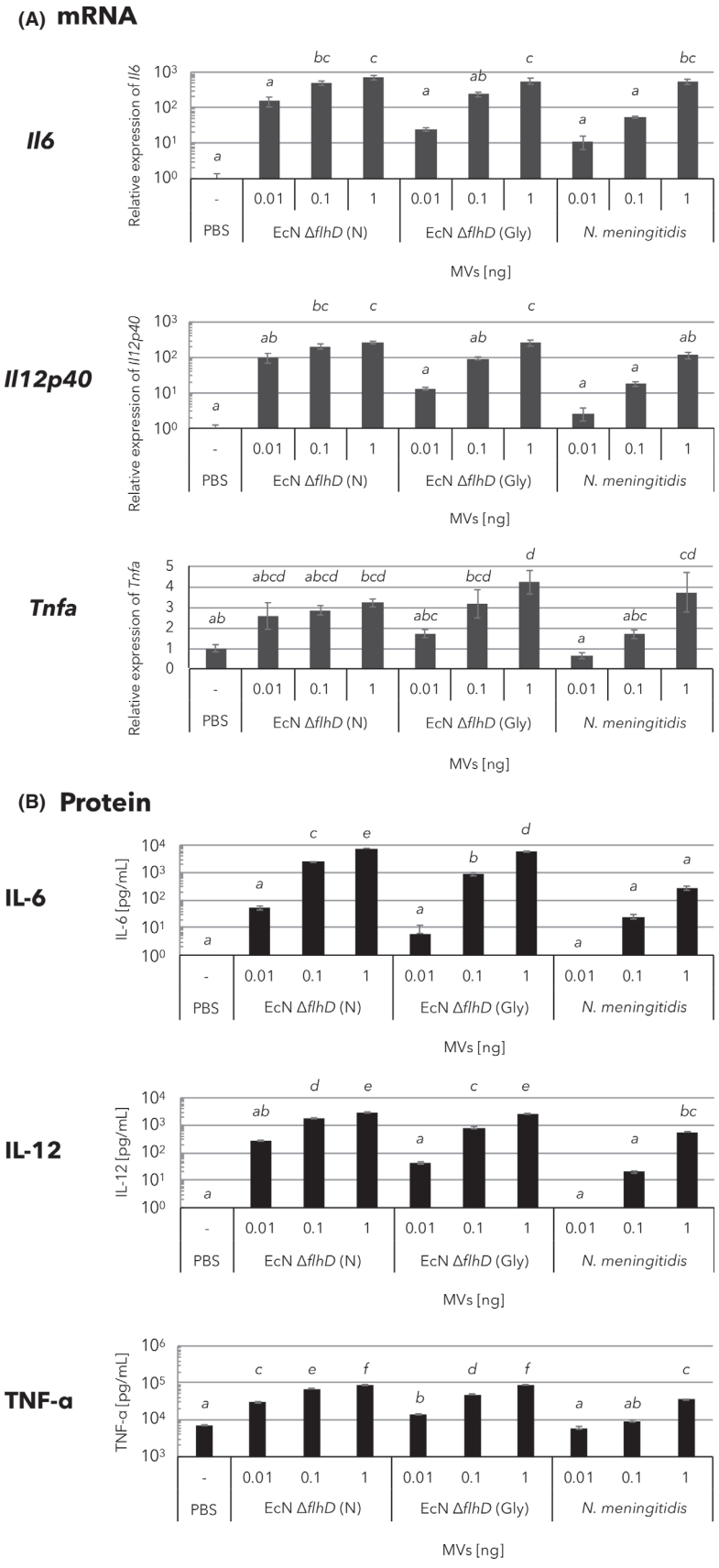

Fig. 5. Cytokine expression of murine macrophage-like cells after treatment with glycine-induced EcNΔ*flhD* MVs.
A. Expression of *Il6*, *Il12p40* and *Tnfa* mRNA in J774.1 cells treated with the following MVs: non-induced EcNΔ*flhD* MVs (N), glycine-induced EcNΔ*flhD* MVs (Gly) and *N. meningitidis* MVs. Following incubation of cells with MVs (0.01–1 ng of protein) for 2 h, the mRNA levels of *Il6*, *Il12p40* and *Tnfa* were quantified. Shown are the qPCR data following normalization against the level of *Actb*.
B. Protein expressions of IL-6, IL-12 and TNF-α in J774.1 cells treated with non-induced EcNΔ*flhD* MVs (N), glycine-induced EcNΔ*flhD* MVs (Gly) and *N. meningitidis* MVs. Following incubation of cells with the MVs (0.01–1 ng of protein) for 12 h, expression levels were quantified by cytokine ELISA. Error bars represent the standard error of the mean of three independent experiments. Statistical analysis was performed using ANOVA and Tukey's multiple comparison test. Different alphabet superscripts indicate significant differences ($P < 0.05$).

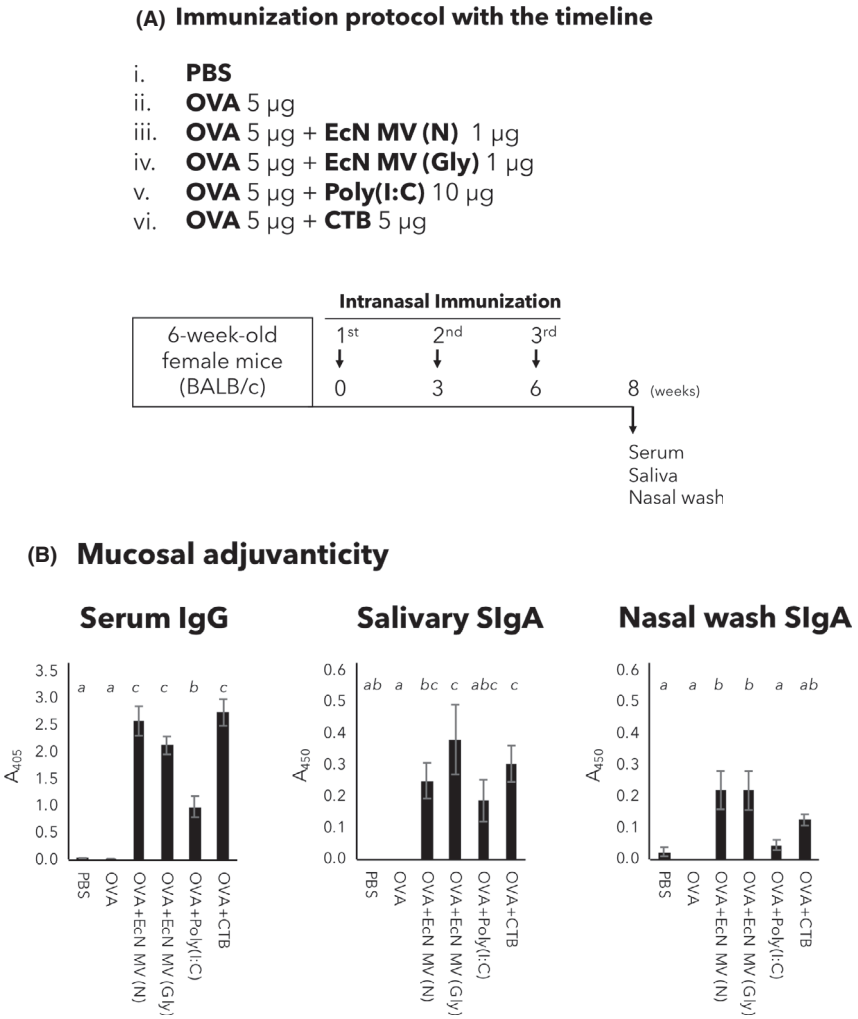

Fig. 6. Assessment of immunomodulatory activity of glycine-induced EcNΔ*flhD* MVs.
(A) Experimental design of intranasal vaccine model study using BALB/c mice. The mucosal adjuvanticity of glycine-induced MVs was examined in this animal study. Female BALB/c mice aged 6 weeks were intranasally immunized three times with the following six conditions ($n = 10$ mice for each group): (i) PBS, mock immunization, (ii) OVA alone, (iii) OVA + non-induced MVs (N), (iv) OVA + glycine-induced MVs (Gly), (v) OVA + Poly(I:C) and (vi) OVA + CTB. At 14 days after the third vaccination, serum, saliva and nasal wash samples were collected from mice. ELISA was carried out to examine OVA-specific serum IgG and IgA, salivary SIgA and nasal wash SIgA.
B. Mucosal adjuvanticity of glycine-induced MVs. At two weeks after the third vaccination, serum, saliva and nasal wash samples were collected from mice intranasally immunized with the following six conditions ($n = 10$ mice for each group): (i) PBS, mock immunization, (ii) OVA alone, (iii) OVA + non-induced MVs (N), (iv) OVA + glycine-induced MVs (Gly), (v) OVA + Poly(I:C) and (vi) OVA + CTB. ELISA was carried out to examine OVA-specific serum IgG, salivary SIgA and nasal wash SIgA. Shown are A_{405} or A_{450} (mean ± SE) values. Samples of serum, saliva and nasal wash were diluted to 1:100, and used as primary antibody of ELISA. All the values except serum IgG were obtained after 60-min incubations with AP or HRP. The value of serum IgG was obtained after a 30 min of incubation with AP. Statistical analysis was performed using ANOVA and Tukey's multiple comparison test. Different alphabet superscripts indicate significant differences ($P < 0.05$).

modified with and without a single O-antigen (O6) repeating unit respectively (Grozdanov *et al*., 2002). Notably, the amount of semi-rough-type LPS was significantly reduced in glycine-induced as compared to non-induced MVs (Fig. 4C).

Glycine-induced MVs showed immunomodulatory activities while reducing endotoxin

To evaluate the immunological properties of different MVs, we first examined the immune responses of the murine macrophage-like cell line J774.1 following addition of different MVs standardized by total protein amounts (Fig. 5). In addition to both non-induced and glycine-induced EcNΔ*flhD* MVs, *Neisseria meningitidis* MVs were also used as a positive control because of their confirmed immunoactivity in humans (Holst *et al*., 2009; Acevedo *et al*., 2014). When compared to PBS used as a vehicle control, the expression level of *Il6* significantly increased in response to all the three MVs tested, when used at 1.0 ng (Fig. 5A, *Il6*), while that of *Il12p40* significantly increased in response to non-induced and glycine-induced EcNΔ*flhD* MVs (Fig. 5A, *Il12p40*), but not neisserial MVs, when used at 1.0 ng. The level of *Tnfa* also increased in response to glycine-induced EcNΔ*flhD* MVs and neisserial MVs at statistically significant levels (Fig. 5A, *Tnfa*), but not by non-induced EcNΔ*flhD* MVs, when used at 1.0 ng. Level of each of the three cytokine mRNAs was increased by all types of MVs in a dose-dependent manner (Fig. 5A). Similar results were obtained with cytokine ELISAs, demonstrating a correlation of the cytokine expression levels between mRNAs in cells and proteins released into the extracellular milieu (Fig. 5B). Together, the levels of the three cytokines following glycine-induced EcNΔ*flhD* MVs were comparable to or higher than those of non-induced EcNΔ*flhD* MVs or neisserial MVs respectively (Fig. 5).

Finally, mucosal adjuvanticity of EcNΔ*flhD* MVs was investigated in our intranasal immunization mouse model (Nakao *et al*., 2011; Nakao *et al*., 2016), according to the protocol shown in Fig. 6A. Humoral immune responses were evaluated by production of the following ovalbumin (OVA)-specific antibodies: serum IgG (total of all IgG subclasses) and IgA, salivary SIgA and nasal wash SIgA (Fig. 6B). Results showed that both non-induced and glycine-induced MVs elicited high levels of all of these OVA-specific antibodies not only in the blood, but also in the nasal and oral cavities, which were comparable and superior to two well-known mucosal adjuvants, cholera toxin B subunit (CTB) and Poly(I:C) respectively. (Fig. 6B). There was no difference in adjuvanticity between non-induced and glycine-induced MVs (Fig. 6B).

Discussion

It is well known that MV preparation from culture supernatant is usually contaminated with a range of bacterial appendages (Ramstedt *et al*., 2011; Nakao *et al*., 2012; Chutkan *et al*., 2013; Nakao *et al*., 2014). Like many other bacteria, abundant flagella were shed from EcN cells into the culture medium, resulting in heavy contamination with flagella in the MV preparation (Fig. 1A). Flagella is one of the virulence factors of *E. coli* and many other bacterial species, as it provides motility (Josenhans and Suerbaum, 2002) and serves as a ligand for TLR5 (Hayashi *et al*., 2001). Here, we could completely circumvent the problem of flagella contamination by eliminating flagella from MV preparations using a flagella-deficient derivative of EcN (EcNΔ*flhD*), which made it possible to isolate pure MVs by simple ultracentrifugation. As a result, we could evaluate both pro-inflammatory responses (Fig. 5) and adjuvanticity (Fig. 6) of flagella-free MVs by excluding the influence of flagella.

Furthermore, we have developed an extraordinarily efficient way to isolate flagella-free EcN MVs by utilizing glycine, an amino acid commonly consumed by humans. Physiologically excessive amounts of glycine (1.0%) induced deformation of the *E. coli* cells (Fig. 2B), indicating loss of integrity of the bacterial cell wall. Along with the cellular deformation, small-sized MVs emerged even at the early exponential growth phase (3 h, Fig. 2C). Very quick turnover of the PG layer of *E. coli* (Olden *et al*., 1975) may accelerate alteration of PG composition by substitution of glycine for DL-alanine of PG (Hammes *et al*., 1973; de Jonge *et al*., 1996). Later on, quasi-lysis occurred along with production of large MVs during the stationary phase growth (Fig. 2B). SEM analysis revealed that large membrane blebs emerged mainly at the cell pole or around the septum during cell division (red arrowheads, Fig. 2B), which is similar to a phenomenon described in a previous report regarding unusual vesicle formation at cell division site of an outer membrane-compromised *E. coli* clone (Sutterlin *et al*., 2016). Taken together, we assume that glycine induced production of small MVs from the early exponential growth phase probably via membrane blebbing, while production of large MVs takes place only during stationary phase growth, which may be associated with cell lysis and/or an abnormal cell division process. The mechanism behind glycine-mediated vesiculogenesis was in good agreement with previous reports of vesiculogenesis in which turnover or degradation of PG is involved (McBroom *et al*., 2006; Schwechheimer *et al*., 2015; Turnbull *et al*., 2016).

In both TEM and SEM analyses, some filamentous structures thinner than flagella were also found in the MV preparations (white arrowheads, Figs 1A and 2C).

The EcN strain carries an inactive P-fimbrial operon and lacks S fimbriae (Grozdanov *et al*., 2004; Sun *et al*., 2005), while it expresses type 1 fimbriae (Stentebjerg-Olesen *et al*., 1999), F1C fimbriae (Lasaro *et al*., 2009) and curli fimbriae (Monteiro *et al*., 2009). Therefore, the filamentous structures observed in the MV preparations were type 1, F1C and/or curli fimbriae. In LC-MS/MS analysis, we confirmed that two different subunits of type 1 fimbriae, FimA and FocG, were contained in the MV preparations (Fig. 4A and Table 1). Of note, fimbriae were tightly associated with MVs (Figs 1A and 2C), which is in good agreement with previous observations of MV preparations from *Porphyromonas gingivalis* (Nakao *et al*., 2014; Bai *et al*., 2015). The presence of fimbria associated with MVs is most likely responsible for MV–host cell interaction, because EcN fimbriae are known to be involved in bacterial adherence, biofilm formation and gut fitness in humans (Lasaro *et al*., 2009; Monteiro *et al*., 2009; Kleta *et al*., 2014). Nevertheless, a definitive conclusion regarding the role of fimbriae in immunomodulatory activity of MVs requires further investigation.

As shown in Fig. 4A and Table 1, more fimbrial proteins were detected as 15-kDa bands in non-induced MVs as compared to glycine-induced conditions. Due to the 69-fold lower yield of non-induced as compared to glycine-induced MVs (Table 1), non-induced MVs were isolated from a much larger culture volume than glycine-induced MVs, which were then subjected to SDS-PAGE and MS analyses. Hence, considering that the amount of fimbriae released into culture supernatant may correlate with cell number, it is not surprising that fimbriae showed greater concentrations in non-induced MV preparations (Fig. 4A and Table 1). Therefore, we would like to call attention to the possible accumulation of bacterial appendages, such as flagella or fimbriae, in MV preparations when concentrated from a large volume of culture supernatant.

In spite of no change in the amount of outer membrane marker protein between glycine-induced and non-induced MVs (Fig. 4B), the former showed significantly lower endotoxin activity (Limulus assay; Fig. 4C). LPS profiling of MVs also revealed that glycine-induced MVs contained much lower levels of semi-rough LPS than non-induced MVs [silver stain and WB (anti-O6); Fig. 4C], suggesting that the lowered endotoxin activity of glycine-induced MVs is mainly due to a reduced amount of semi-rough LPS. In addition, the mechanism behind reduction in semi-rough LPS in glycine-induced MVs may be explained by an effect of glycine on either inhibition of O-antigen ligation to lipid A-core oligosaccharide, or cleavage of O-antigen from semi-rough LPS. Furthermore, given that MV architecture is influenced by an imbalance between semi-rough LPS and rough LPS, glycine-induced changes in the morphology (Fig. 3) and protein constituents (Fig. 5A and B) of MVs may be associated with the stoichiometric distribution of different LPS species.

The amount of LPS per protein in the glycine-induced MVs was unexpectedly eightfold less than that in non-induced MVs. On the other hand, the glycine-induced MVs efficiently elicited host immune responses in both in vitro and in vivo studies (Figs 5 and 6). In general, MVs contain abundant LPS, which is known to induce a pyrogenic response and ultimately trigger septic shock. However, mucosal administration of LPS, apart from the parenteral administration, is thought to be safe in humans (Illyes *et al*., 2008; Inagawa *et al*., 2011). The established safety of an oral probiotics, Mutaflor, is a good example of LPS safety, because Mutaflor contains 2.5–25 $\times$ 10^9 CFU of EcN per capsule, and thus contains plenty of LPS. Nevertheless, the mucosal administration of LPS-reduced MVs could be safer than LPS-enriched MVs in the event that a wound is accidentally created at the mucosal surface during MV administration. In addition, removal of bacterial endotoxin from *E. coli*-derived products is a time-consuming and expensive process that is frequently required for the safety of the final product. Therefore, we are excited that this promising method can isolate LPS-reduced EcN MVs, which would be applicable especially for use as vaccines and adjuvants in humans.

In general, LPS is one of the major constituents of MVs derived from Gram-negative bacteria, and the lipid A portion of LPS plays a central role in the host immune responses through TLR4-mediated signalling (Miller *et al*., 2005). For example, TLR4 activation contributes to the immunogenicity of the *N. meningitidis* MV vaccine in a mouse model (Fransen *et al*., 2010). On the other hand, *Salmonella typhimurium* MVs stimulate dendritic cells through not only TLR4-dependent, but also TLR4-independent signalling (Alaniz *et al*., 2007). *P. gingivalis* MVs show differential immune responses via TLR2, TLR4, TLR7, TLR8 and TLR9 (Cecil *et al*., 2016). Sturm *et al*. reported that EcN-derived secreted factors (probably containing MVs) modulate T-cell activation via TLR2 signalling (Sturm *et al*., 2005). In the present study, the immunoactivity of glycine-induced EcNΔ*flhD* MVs was shown to be comparable to that of non-induced MVs (Figs 5 and 6). The finding indicates that the immune modulatory activities of glycine-induced EcNΔ*flhD* MVs are dependent on signalling via MV-derived agonist(s) other than LPS (TLR4 agonist) or flagellin (TLR5 agonist). For example, agonists of TLR2 (lipoproteins), TLR7 (single-stranded RNA), TLR9 (CpG DNA) and/or NOD1/NOD2 (peptidoglycans) may be involved in these immune modulatory activities. Further analysis is required to elucidate the immunological factor(s) in EcN MVs involved in these activities.

Biologically active nanoparticles would be applicable as immunotherapeutic tools such as vaccines and adjuvants against not only a wide range of infectious diseases (Kaparakis-Liaskos and Ferrero, 2015), but also many other diseases including cancers and allergic diseases (Kishimoto and Maldonado, 2018; Ke *et al*., 2019). Among various possible nanoparticle-based vaccines, bacterial MVs could be developed as novel drug delivery systems for use in medical and healthcare settings. Furthermore, new generations of semi-synthetic MVs are emerging through innovative bioengineering technology (Rosenthal *et al*., 2014; Stevenson *et al*., 2018). On the basis of these findings, we suggest that glycine-induced EcNΔ*flhD* MVs are applicable as a novel vaccine delivery platform that provides low vaccine reactogenicity and high adjuvanticity and immunogenicity.

Experimental procedures

Strains and culture condition

The *E. coli* probiotic strain EcN (DSM 6601, serotype O6:K5:H1), its flagella-deficient derivative (EcNΔ*flhD*) and the Δ*flhD* mutant of *E. coli* BW25113 (K-12 strain, National BioResource Project-*E. coli* in National Institute of Genetics, Japan) were used in this study. *Neisseria meningitidis* strain H44/76 (Holten, 1979) was also used in this study. All *E. coli* strains were grown either in liquid LB broth or on solid medium at 37 °C in aerobic conditions. The *N. meningitidis* strain was grown on agar plates with a GC medium base (Becton Dickinson, Franklin Lakes, NJ, USA), supplemented with 1% IsoVitaleX (Becton Dickinson) at 37 °C in aerobic conditions. To evaluate the effects of glycine, precultured seeds were inoculated at a dilution of 1:200 into fresh LB broth supplemented with glycine at different concentrations, and incubated at 37 °C with shaking, and growth curves were generated by sequential measurement of OD at 660 nm using a bio-photorecorder (TVS062CA, Advantec, Tokyo, Japan).

*Constructions of EcNΔ*flhD

Deletion of the *flhD* gene in the chromosome of EcN was conducted according to the method of Datsenko and Wanner (Datsenko and Wanner, 2000) using primers with homologous sequences to the *flhD* and Km^R genes of the pKD4 plasmid, which are described in the study of Baba *et al.* (2006). The *flhD* gene was replaced with a Km^R cassette, followed by elimination of the cassette by FLP recombinase (Datsenko and Wanner, 2000).

MV preparations

Membrane vesicles were purified as described previously, with some modifications (Nakao *et al*., 2011; Nakao *et al*., 2016). Briefly, the EcN wild-type and the Δ*flhD* mutant strains were separately cultured in LB broth with or without extra glycine at 37 °C for 16 h with shaking. Supernatants were collected by centrifugation at 7190 × *g* for 30 min at 4 °C, then filtered through a 0.45-μm pore-sized filter (Merck, Darmstadt, Germany) and ultracentrifuged at 103 800 × *g* for 2 h at 4 °C. The resulting MV fraction pellets were suspended in 20 mM Tris-HCl (pH 8.0). In some experiments, MV preparations of EcN wild-type strain were subjected to further purification using density gradient centrifugation separation, as described previously (Chutkan *et al*., 2013), to try to eliminate contamination of flagella from the MV preparations.

Measurement of the MV quantity and particle size

Protein concentration in the MV suspensions was determined using a Bradford assay, with bovine serum albumin as the standard. Lipid concentration in the MV suspensions was determined using FM4-64 dye (Life Technologies, Carlsbad, CA, USA), with water-soluble linoleic acid (Sigma, St. Louis, MO, USA) as the standard. Standards and samples (5 μl) were mixed with 100 μl of 5 μg ml^{-1} FM4-64 in the 96-well black plate, and incubated for 10 min at room temperature. Fluorescence from FM4-64 (excitation at 535 nm and emission at 625 nm) was detected with the plate reader Cytation5 (Biotek, Winooski, VT, USA). Limulus assay was performed to quantify LPS using an Endospecy ES-50M kit (Seikagaku Co., Tokyo, Japan) according to the manufacturers' instructions, with LPS from *Escherichia coli* O111:B4 (Sigma) as the standard. MV particle size was measured from TEM images using the Fiji image processing package (a variant of ImageJ) (Schindelin *et al*., 2012).

SDS-PAGE and Western blotting

SDS-PAGE and Western blotting were performed as described previously (Nakao *et al*., 2012), with some modifications. MV and whole-cell samples were separated by Tris-glycine SDS-PAGE using 12.5% polyacrylamide gels and stained with Coomassie brilliant blue (CBB). For Western blotting, gels were electroblotted onto PVDF membranes. Rabbit polyclonal antibodies against flagellin of *E. coli* (FliC) (Pouttu *et al*., 2001) and representative proteins localized in the outer membrane (OmpC) (Nakao *et al*., 2012), inner membrane (RodZ, provided by NBRP-*E. coli* at NIG) and cytosol (Crp) (Nakao *et al*., 2012) were used at dilutions of 1:1600, 1:400, 1:400 and 1:1000. Two different molecular weights of LPS bands (Grozdanov *et al*., 2002) were separated by Tris-tricine SDS-PAGE using 16.5%

polyacrylamide gels, and determined by silver stain (Tsai and Frasch, 1982), as well as Western blot using rabbit polyclonal antibodies against *E. coli* O6 antiserum (85002, SSI Diagnostica, Hillerød, Denmark). The O6 antiserum was used at dilution of 1:50,000. Horseradish peroxidase-labelled anti-rabbit IgG (GE Healthcare, Buckinghamshire, UK) was used as the secondary antibody at a dilution of 1:200 000. Following addition of the substrate, chemiluminescence was visualized with a FUSION SOLO.7S.EDGE (Vilber Lourmat, Marne-la-Vallée, France).

Protein identification by LC-MS/MS

Following SDS-PAGE, CBB-stained protein bands were excised and subjected to in-gel digestion with sequencing grade modified trypsin (Promega, Madison, WI, USA) as previously described (Bahk *et al*., 2004). Briefly, the resulting tryptic peptides were separated and analysed using reversed-phase capillary HPLC directly coupled to a Finnigan LCQ ion trap mass spectrometer (LC-MS/MS) (Zuo *et al*., 2001, with a slight modification). Both a 0.1 × 20 mm trapping column and a 0.075 × 130 mm resolving column were packed with Vydac 218MS low trifluoroacetic acid C18 beads (5 μm in size, pore size 300 Å; Vydac, Hesperia, CA, USA) and placed in-line. Next, the peptides were bound to the trapping column for 10 min with 5% (v/v) aqueous acetonitrile containing 0.1% (v/v) formic acid; then, bound peptides were eluted with a 50 min gradient of 5–80% (v/v) acetonitrile containing 0.1% (v/v) formic acid at a flow rate of 0.2 μl min^{-1}. For tandem mass spectrometry, the full mass scan range mode was m/z = 450–2000 Da. After determination of the charge states of ions in zoom scans, product ion spectra were acquired in MS/MS mode with a relative collision energy of 55%. Individual spectra from MS/MS were processed using the TurboSEQUEST software package (Thermo Quest, San Jose, CA, USA). Generated peak list files were used to query the NCBIprot database, using the MASCOT program (http://www.matrixscience.com/cgi/search_form.pl?FORMVER=2&SEARCH=PMF).
Peptide mass tolerance for Mascot analysis was set at modifications of methionine and cysteine, peptide mass tolerance of 2 Da, MS/MS ion mass tolerance of 0.8 Da, allowance of missed cleavage at 2 and charge states (+1, +2, +3). PSORTb ver. 3.0.2 (https://www.psort.org/psortb/), SignalP ver. 4.1 (http://www.cbs.dtu.dk/services/SignalP/), LipoP ver. 1.0 (http://www.cbs.dtu.dk/services/LipoP/) and Compute pI/Mw Tool of ExPASy (https://web.expasy.org/compute_pi/) were the applications used for predicting subcellular localization, presence and location of signal peptide cleavage sites in the amino acid sequences, and theoretical pI (isoelectric point)/MW (molecular weight) respectively.

TEM and SEM

TEM observation of MVs was conducted as previously described (Bai *et al*., 2015). SEM observations of cells were conducted as previously described, with some modifications (Nakao *et al*., 2011). Briefly, bacterial cell suspension was fixed with 5% glutaraldehyde and 4% paraformaldehyde in PBS at the ratio of 1:1. The preparation was placed on poly-L-lysine-coated coverslips for 16 h to allow the cells to attach. After washing three times with PBS, the samples were dehydrated in graded acetone solutions, and dried in a critical point dryer using CO_2 (CPD 030, BAL-TEC AG, Balzers, Liechtenstein, Germany). The samples were then coated with osmium vapour using an osmium plasma coater and finally visualized with SEM (Regulus8220, Hitachi High-Technologies, Tokyo, Japan).

Cytokine expression in murine macrophage-like cells

Quantification of *Il6*, *Il12p40* and *Tnfa* mRNAs in J774.1 cells was conducted by qPCR as previously described, with some modifications (Nakao *et al*., 2016). Expressions of the cytokines IL-6, IL-12 and TNF-α in J774.1 cells were also quantified by using an enzyme-linked immunosorbent assay (ELISA) as described previously (Obana *et al*., 2017). Briefly, cells from the mouse macrophage-like cell line J774.1 were grown in RPMI 1640 medium (Sigma), supplemented with 10% heat-inactivated fetal calf serum, 100 units ml^{-1} of penicillin and 0.1 mg ml^{-1} streptomycin at 37°C in a humidified atmosphere containing 5% CO_2. Cells (6.6×10^5) were then incubated with MVs for 2 or 12 h. Whole cells were collected after 2 h and used for RNA extraction and cDNA synthesis, performed using an RNeasy Mini Kit (Qiagen, Hilden, Germany) and ReverTra Ace qPCR RT Master Mix with gDNA Remover (Toyobo, Tokyo, Japan), respectively, according to the manufacturers' instructions. TaqMan qPCR was performed using an Applied Biosystems 7500 Fast Real-Time PCR System (Thermo Fisher Scientific, Waltham, MA, USA) with Premix Ex Taq (Probe qPCR) (Takara Bio, Shiga, Japan). The mRNA levels of *Il6*, *Il12p40*, *Tnfa* and *Actb* were quantified by qPCR using specific primer pairs and probes, as previously described (Ichinohe *et al*., 2005). The expression levels of *Il6*, *Il12p40* and *Tnfa* mRNA in each sample were normalized to those of *Actb* mRNA. Culture supernatants collected at 12 h were used for detection of IL-6, IL-12 and TNF-α with sandwich ELISA kits (900-M50, 900-M97, 900-M54; PeproTech, Rocky Hill, NJ, USA). MVs of *N. meningitidis* H44/76 were also used as a positive control. Meningococcal MVs were harvested from confluent-grown bacteria on agar plates.

Immunization and ELISA

All animal experiments were approved by our Institutional Animal Care and Use Committee (Protocol No.: 118059), and performed in compliance with our institutional guidelines. In Fig. 6A, the experimental design is shown with the timeline of OVA immunization with or without different adjuvants. Female BALB/c mice (Japan SLC, Inc, Hamamatsu, Japan) aged 6 weeks were intranasally immunized three times at three weeks of intervals by dropping 10 μl into nostrils (5 μl each) with 5 μg of ovalbumin (OVA; Sigma) alone or 5 μg of OVA with the following materials: 1 μg of non-induced MVs, 1 μg of glycine-induced MVs, polyriboinosinic polyribocytidylic acid (Poly[I:C]; Sigma) and cholera toxin B subunit (CTB; Wako). At two weeks after the third immunization, sera, nasal washes and saliva specimens were collected and used for ELISA, as described previously (Nakao *et al*., 2011) except for the procedure of antigen coating, in which OVA antigen at 10 μg per well was coated onto ELISA plates. Alkaline phosphatase (AP)-labelled anti-mouse IgG (H + L) (A16069, Thermo Fisher Scientific, San Jose, CA, USA) and horseradish peroxidase (HRP)-labelled anti-mouse IgA (14-18-01, KPL, Gaithersburg, MD, USA) were used at 1:1000 dilutions. OVA-specific antibodies were detected by chromogenic development using para-nitrophenyl phosphate and 3,5,3',5'-tetramethylbenzidine as the substrates for AP and HRP respectively. The reaction of HRP was stopped by 1N HCl. Absorbance at 405 and 450 nm was measured to detect enzyme reactions of AP and HRP respectively.

Statistical analysis

Statistical analysis was performed using unpaired *t*-test with Welch's correction, Mann–Whitney's *U*-test or one-way analysis of variance (ANOVA) followed by Tukey's multiple comparison test. *P*-values of 0.05 or lower were considered to be statistically significant.

Acknowledgements

We thank Michiyo Kataoka, Hirotaka Kobayashi, Fumiko Takashima and Junko Sugita for their technical assistance. We also thank Haruo Watanabe, Hidenobu Senpuku and Makoto Ohnishi for their helpful comments and discussion. Some materials were provided by Bernt Eric Uhlin, Sunao Iyoda, Hideyuki Takahashi, Akira Ainai and NBRP-*E. coli* at NIG, Japan. This study was supported by a grant from the Japan Agency for Medical Research and Development (AMED, no. JP18fk0108124) and JSPS KAKENHI (JP16K11537, JP18K15160, JP19H02920 and JP19K22644).

Conflict of interest

None declared.

Author contributions

S.H. conducted all of the experiments described in the manuscript. S.H. and R.N. conceived the experiments, interpreted the results and wrote the manuscript.

References

Acevedo, R., Fernandez, S., Zayas, C., Acosta, A., Sarmiento, M.E., Ferro, V.A., *et al*. (2014) Bacterial outer membrane vesicles and vaccine applications. *Front Immunol* **5:** 121.

Aguilera, L., Toloza, L., Gimenez, R., Odena, A., Oliveira, E., Aguilar, J., *et al*. (2014) Proteomic analysis of outer membrane vesicles from the probiotic strain *Escherichia coli* Nissle 1917. *Proteomics* **14:** 222–229.

Alaniz, R.C., Deatherage, B.L., Lara, J.C., and Cookson, B.T. (2007) Membrane vesicles are immunogenic facsimiles of *Salmonella typhimurium* that potently activate dendritic cells, prime B and T cell responses, and stimulate protective immunity in vivo. *J Immunol* **179:** 7692–7701.

Baba, T., Ara, T., Hasegawa, M., Takai, Y., Okumura, Y., Baba, M., *et al*. (2006) Construction of *Escherichia coli* K-12 in-frame, single-gene knockout mutants: the Keio collection. *Mol Syst Biol* **2:** 2006 0008.

Bahk, Y.Y., Kim, S.A., Kim, J.S., Euh, H.J., Bai, G.H., Cho, S.N., and Kim, Y.S. (2004) Antigens secreted from *Mycobacterium tuberculosis*: identification by proteomics approach and test for diagnostic marker. *Proteomics* **4:** 3299–3307.

Bai, D., Nakao, R., Ito, A., Uematsu, H., and Senpuku, H. (2015) Immunoreactive antigens recognized in serum samples from mice intranasally immunized with *Porphyromonas gingivalis* outer membrane vesicles. *Pathog Dis* **73:** pii: ftu006.

Beckham, K.S., Connolly, J.P., Ritchie, J.M., Wang, D., Gawthorne, J.A., Tahoun, A., *et al*. (2014) The metabolic enzyme AdhE controls the virulence of *Escherichia coli* O157:H7. *Mol Microbiol* **93:** 199–211.

Behnsen, J., Deriu, E., Sassone-Corsi, M., and Raffatellu, M. (2013) Probiotics: properties, examples, and specific applications. *Cold Spring Harb Perspect Med* **3:** a010074.

Beringer, J.E. (1974) R factor transfer in *Rhizobium leguminosarum*. *J Gen Microbiol* **84:** 188–198.

Boutriau, D., Poolman, J., Borrow, R., Findlow, J., Domingo, J.D., Puig-Barbera, J., *et al*. (2007) Immunogenicity and safety of three doses of a bivalent (B:4:p1.19,15 and B:4:p1.7-2,4) meningococcal outer membrane vesicle vaccine in healthy adolescents. *Clin Vaccine Immunol* **14:** 65–73.

Cecil, J.D., O'Brien-Simpson, N.M., Lenzo, J.C., Holden, J.A., Chen, Y.Y., Singleton, W., *et al*. (2016) Differential responses of pattern recognition receptors to outer membrane vesicles of three periodontal pathogens. *PLoS ONE* **11:** e0151967.

Chatterjee, B.R., and Williams, R.P. (1963) Preparation of Spheroplasts from *Vibrio Comma*. *J Bacteriol* **85:** 838–841.

Chutkan, H., Macdonald, I., Manning, A., and Kuehn, M.J. (2013) Quantitative and qualitative preparations of bacterial outer membrane vesicles. *Methods Mol Biol* **966:** 259–272.

Clark, D.P., and Cronan, J.E. Jr (1980) Acetaldehyde coenzyme A dehydrogenase of *Escherichia coli*. *J Bacteriol* **144:** 179–184.

Datsenko, K.A., and Wanner, B.L. (2000) One-step inactivation of chromosomal genes in *Escherichia coli* K-12 using PCR products. *Proc Natl Acad Sci USA* **97:** 6640–6645.

European Commission. (2014) *Food additives* [WWW document]. URL https://www.efsa.europa.eu/en/efsajournal/pub/3670.

Fabrega, M.J., Aguilera, L., Gimenez, R., Varela, E., Alexandra Canas, M., Antolin, M., *et al*. (2016) Activation of immune and defense responses in the intestinal mucosa by outer membrane vesicles of commensal and probiotic *Escherichia coli* strains. *Front Microbiol* **7:** 705.

Fransen, F., Stenger, R.M., Poelen, M.C., van Dijken, H.H., Kuipers, B., Boog, C.J., *et al*. (2010) Differential effect of TLR2 and TLR4 on the immune response after immunization with a vaccine against *Neisseria meningitidis* or *Bordetella pertussis*. *PLoS ONE* **5:** e15692.

Grozdanov, L., Zahringer, U., Blum-Oehler, G., Brade, L., Henne, A., Knirel, Y.A., *et al*. (2002) A single nucleotide exchange in the wzy gene is responsible for the semirough O6 lipopolysaccharide phenotype and serum sensitivity of *Escherichia coli* strain Nissle 1917. *J Bacteriol* **184:** 5912–5925.

Grozdanov, L., Raasch, C., Schulze, J., Sonnenborn, U., Gottschalk, G., Hacker, J., and Dobrindt, U. (2004) Analysis of the genome structure of the nonpathogenic probiotic *Escherichia coli* strain Nissle 1917. *J Bacteriol* **186:** 5432–5441.

Hammes, W., Schleifer, K.H., and Kandler, O. (1973) Mode of action of glycine on the biosynthesis of peptidoglycan. *J Bacteriol* **116:** 1029–1053.

Hayashi, F., Smith, K.D., Ozinsky, A., Hawn, T.R., Yi, E.C., Goodlett, D.R., *et al*. (2001) The innate immune response to bacterial flagellin is mediated by Toll-like receptor 5. *Nature* **410:** 1099–1103.

Holo, H., and Nes, I.F. (1989) High-frequency transformation, by electroporation, of *Lactococcus lactis* subsp. cremoris grown with glycine in osmotically stabilized media. *Appl Environ Microbiol* **55:** 3119–3123.

Holst, J., Martin, D., Arnold, R., Huergo, C.C., Oster, P., O'Hallahan, J., and Rosenqvist, E. (2009) Properties and clinical performance of vaccines containing outer membrane vesicles from *Neisseria meningitidis*. *Vaccine* **27 (Suppl** 2): B3–B12.

Holten, E. (1979) Serotypes of *Neisseria meningitidis* isolated from patients in Norway during the first six months of 1978. *J Clin Microbiol* **9:** 186–188.

Ichinohe, T., Watanabe, I., Ito, S., Fujii, H., Moriyama, M., Tamura, S., *et al*. (2005) Synthetic double-stranded RNA poly(I:C) combined with mucosal vaccine protects against influenza virus infection. *J Virol* **79:** 2910–2919.

Illyes, G., Kovacs, K., Kocsis, B., and Baintner, K. (2008) Failure of oral *E. coli* O83 lipopolysaccharide to influence intestinal morphology and cell proliferation in rats: short communication. *Acta Vet Hung* **56:** 1–3.

Inagawa, H., Kohchi, C., and Soma, G. (2011) Oral administration of lipopolysaccharides for the prevention of various diseases: benefit and usefulness. *Anticancer Res* **31:** 2431–2436.

Ito, M., and Nagane, M. (2001) Improvement of the electrotransformation efficiency of facultatively alkaliphilic *Bacillus pseudofirmus* OF4 by high osmolarity and glycine treatment. *Biosci Biotechnol Biochem* **65:** 2773–2775.

John, R.V., and Russell, A.D. (1963) The antibacterial action of glycine. *J Pharm Pharmacol* **15:** 346–347.

de Jonge, B.L., Chang, Y.S., Xu, N., and Gage, D. (1996) Effect of exogenous glycine on peptidoglycan composition and resistance in a methicillin-resistant *Staphylococcus aureus* strain. *Antimicrob Agents Chemother* **40:** 1498–1503.

Josenhans, C., and Suerbaum, S. (2002) The role of motility as a virulence factor in bacteria. *Int J Med Microbiol* **291:** 605–614.

Kaparakis-Liaskos, M., and Ferrero, R.L. (2015) Immune modulation by bacterial outer membrane vesicles. *Nat Rev Immunol* **15:** 375–387.

Ke, X., Howard, G.P., Tang, H., Cheng, B., Saung, M.T., Santos, J.L., and Mao, H.Q. (2019) Physical and chemical profiles of nanoparticles for lymphatic targeting. *Adv Drug Deliv Rev* **151–152:** 72–93.

Kishimoto, T.K., and Maldonado, R.A. (2018) Nanoparticles for the induction of antigen-specific immunological tolerance. *Front Immunol* **9:** 230.

Kleta, S., Nordhoff, M., Tedin, K., Wieler, L.H., Kolenda, R., Oswald, S., *et al*. (2014) Role of F1C fimbriae, flagella, and secreted bacterial components in the inhibitory effect of probiotic *Escherichia coli* Nissle 1917 on atypical enteropathogenic *E. coli* infection. *Infect Immun* **82:** 1801–1812.

Kruis, W., Fric, P., Pokrotnieks, J., Lukas, M., Fixa, B., Kascak, M., *et al*. (2004) Maintaining remission of ulcerative colitis with the probiotic *Escherichia coli* Nissle 1917 is as effective as with standard mesalazine. *Gut* **53:** 1617–1623.

Larsen, M.H., Biermann, K., Tandberg, S., Hsu, T., and Jacobs, W.R. Jr (2007) Genetic manipulation of *Mycobacterium tuberculosis*. *Curr Protoc Microbiol* Chapter 10: Unit 10A 12.

Lasaro, M.A., Salinger, N., Zhang, J., Wang, Y., Zhong, Z., Goulian, M., and Zhu, J. (2009) F1C fimbriae play an important role in biofilm formation and intestinal colonization by the *Escherichia coli* commensal strain Nissle 1917. *Appl Environ Microbiol* **75:** 246–251.

van der Ley, P., and van den Dobbelsteen, G. (2011) Next-generation outer membrane vesicle vaccines against *Neisseria meningitidis* based on nontoxic LPS mutants. *Hum Vaccine* **7:** 886–890.

van der Pol, L., Stork, M., and van der Ley, P. (2015) Outer membrane vesicles as platform vaccine technology. *Biotechnol J* **10:** 1689–1706.

McBroom, A.J., Johnson, A.P., Vemulapalli, S., and Kuehn, M.J. (2006) Outer membrane vesicle production by

Escherichia coli is independent of membrane instability. *J Bacteriol* **188:** 5385–5392.

Miller, S.I., Ernst, R.K., and Bader, M.W. (2005) LPS, TLR4 and infectious disease diversity. *Nat Rev Microbiol* **3:** 36–46.

Monteiro, C., Saxena, I., Wang, X., Kader, A., Bokranz, W., Simm, R., *et al*. (2009) Characterization of cellulose production in *Escherichia coli* Nissle 1917 and its biological consequences. *Environ Microbiol* **11:** 1105–1116.

Nakao, R., Hasegawa, H., Ochiai, K., Takashiba, S., Ainai, A., Ohnishi, M., *et al*. (2011) Outer membrane vesicles of *Porphyromonas gingivalis* elicit a mucosal immune response. *PLoS ONE* **6:** e26163.

Nakao, R., Ramstedt, M., Wai, S.N., and Uhlin, B.E. (2012) Enhanced biofilm formation by *Escherichia coli* LPS mutants defective in Hep biosynthesis. *PLoS ONE* **7:** e51241.

Nakao, R., Kikushima, K., Higuchi, H., Obana, N., Nomura, N., Bai, D., *et al*. (2014) A novel approach for purification and selective capture of membrane vesicles of the periodontopathic bacterium, *Porphyromonas gingivalis*: membrane vesicles bind to magnetic beads coated with epoxy groups in a noncovalent, species-specific manner. *PLoS ONE* **9:** e95137.

Nakao, R., Hasegawa, H., Dongying, B., Ohnishi, M., and Senpuku, H. (2016) Assessment of outer membrane vesicles of periodontopathic bacterium *Porphyromonas gingivalis* as possible mucosal immunogen. *Vaccine* **34:** 4626–4634.

Obana, N., Nakao, R., Nagayama, K., Nakamura, K., Senpuku, H., and Nomura, N. (2017) Immunoactive clostridial membrane vesicle production is regulated by a sporulation factor. *Infect Immun* **85:** pii: e00096-17.

Olden, K., Ito, S., and Wilson, T.H. (1975) D-Alanine-requiring cell wall mutant of *Escherichia coli*. *J Bacteriol* **122:** 1310–1321.

Pouttu, R., Westerlund-Wikstrom, B., Lang, H., Alsti, K., Virkola, R., Saarela, U., *et al*. (2001) matB, a common fimbrillin gene of *Escherichia coli*, expressed in a genetically conserved, virulent clonal group. *J Bacteriol* **183:** 4727–4736.

Ramstedt, M., Nakao, R., Wai, S.N., Uhlin, B.E., and Boily, J.F. (2011) Monitoring surface chemical changes in the bacterial cell wall: multivariate analysis of cryo-x-ray photoelectron spectroscopy data. *J Biol Chem* **286:** 12389–12396.

Rembacken, B.J., Snelling, A.M., Hawkey, P.M., Chalmers, D.M., and Axon, A.T. (1999) Non-pathogenic *Escherichia coli* versus mesalazine for the treatment of ulcerative colitis: a randomised trial. *Lancet* **354:** 635–639.

Rosenthal, J.A., Huang, C.J., Doody, A.M., Leung, T., Mineta, K., Feng, D.D., *et al*. (2014) Mechanistic insight into the TH1-biased immune response to recombinant subunit vaccines delivered by probiotic bacteria-derived outer membrane vesicles. *PLoS ONE* **9:** e112802.

Sassone-Corsi, M., Nuccio, S.P., Liu, H., Hernandez, D., Vu, C.T., Takahashi, A.A., *et al*. (2016) Microcins mediate competition among Enterobacteriaceae in the inflamed gut. *Nature* **540:** 280–283.

Sato, H., Diena, B.B., and Greenberg, L. (1966) Spheroplast induction and lysis of BCG strains by glycine and lysozyme. *Can J Microbiol* **12:** 255–261.

Schindelin, J., Arganda-Carreras, I., Frise, E., Kaynig, V., Longair, M., Pietzsch, T., *et al*. (2012) Fiji: an open-source platform for biological-image analysis. *Nat Methods* **9:** 676–682.

Schwechheimer, C., and Kuehn, M.J. (2015) Outer-membrane vesicles from Gram-negative bacteria: biogenesis and functions. *Nat Rev Microbiol* **13:** 605–619.

Schwechheimer, C., Rodriguez, D.L., and Kuehn, M.J. (2015) NlpI-mediated modulation of outer membrane vesicle production through peptidoglycan dynamics in *Escherichia coli*. *Microbiologyopen* **4:** 375–389.

Shibasaki, I. (1982) Food preservation with nontraditional antimicrobial agents. *J Food Saf* **4:** 35–38.

Soutourina, O.A., and Bertin, P.N. (2003) Regulation cascade of flagellar expression in Gram-negative bacteria. *FEMS Microbiol Rev* **27:** 505–523.

Stentebjerg-Olesen, B., Chakraborty, T., and Klemm, P. (1999) Type 1 fimbriation and phase switching in a natural *Escherichia coli* fimB null strain, Nissle 1917. *J Bacteriol* **181:** 7470–7478.

Stevenson, T.C., Cywes-Bentley, C., Moeller, T.D., Weyant, K.B., Putnam, D., Chang, Y.F., *et al*. (2018) Immunization with outer membrane vesicles displaying conserved surface polysaccharide antigen elicits broadly antimicrobial antibodies. *Proc Natl Acad Sci USA* **115:** E3106–E3115.

Sturm, A., Rilling, K., Baumgart, D.C., Gargas, K., Abou-Ghazale, T., Raupach, B., *et al*. (2005) *Escherichia coli* Nissle 1917 distinctively modulates T-cell cycling and expansion via toll-like receptor 2 signaling. *Infect Immun* **73:** 1452–1465.

Sun, J., Gunzer, F., Westendorf, A.M., Buer, J., Scharfe, M., Jarek, M., *et al*. (2005) Genomic peculiarity of coding sequences and metabolic potential of probiotic *Escherichia coli* strain Nissle 1917 inferred from raw genome data. *J Biotechnol* **117:** 147–161.

Sutterlin, H.A., Shi, H., May, K.L., Miguel, A., Khare, S., Huang, K.C., and Silhavy, T.J. (2016) Disruption of lipid homeostasis in the Gram-negative cell envelope activates a novel cell death pathway. *Proc Natl Acad Sci USA* **113:** E1565–E1574.

Thompson, K., and Collins, M.A. (1996) Improvement in electroporation efficiency for *Lactobacillus plantarum* by the inclusion of high concentrations of glycine in the growth medium. *J Microbiol Methods* **26:** 73–79.

Toyofuku, M. (2019) Bacterial communication through membrane vesicles. *Biosci Biotechnol Biochem* **83:** 1599–1605.

Toyofuku, M., Tashiro, Y., Hasegawa, Y., Kurosawa, M., and Nomura, N. (2015) Bacterial membrane vesicles, an overlooked environmental colloid: biology, environmental perspectives and applications. *Adv Colloid Interface Sci* **226:** 65–77.

Tsai, C.M., and Frasch, C.E. (1982) A sensitive silver stain for detecting lipopolysaccharides in polyacrylamide gels. *Anal Biochem* **119:** 115–119.

Turnbull, L., Toyofuku, M., Hynen, A.L., Kurosawa, M., Pessi, G., Petty, N.K., *et al*. (2016) Explosive cell lysis as a mechanism for the biogenesis of bacterial membrane vesicles and biofilms. *Nat Commun* **7:** 11220.

U.S. Food and Drug Administration (2018) *Food additive status list* [WWW document]. URL www.fda.gov/food/food-additives-petitions/food-additive-status-list

Wang, W., Chanda, W., and Zhong, M. (2015) The relationship between biofilm and outer membrane vesicles: a novel therapy overview. *FEMS Microbiol Lett* **362:** fnv117.

Zuo, X., Echan, L., Hembach, P., Tang, H.Y., Speicher, K.D., Santoli, D., and Speicher, D.W. (2001) Towards global analysis of mammalian proteomes using sample prefractionation prior to narrow pH range two-dimensional gels and using one-dimensional gels for insoluble and large proteins. *Electrophoresis.* **22(9):** 1603–1615.

Supporting information

Additional supporting information may be found online in the Supporting Information section at the end of the article.
Figure S1. Hirayama and Nakao.
Figure S2. Hirayama and Nakao.
Figure S3. Hirayama and Nakao.

